

Two-dimensional magnetoplasma/Bernstein modes coupled with bulk and surface optical phonons

Norman J. M. Horing

Department of Physics and Engineering Physics, Stevens Institute of Technology, Hoboken, New Jersey 07030

Godfrey Gumbs*

Department of Physics and Astronomy, Hunter College, CUNY, 695 Park Avenue, New York, New York 10021

(Received 18 May 1998)

We analyze the interaction of two-dimensional (2D) magnetoplasmons, including 2D Bernstein modes, with bulk and surface optical phonons. The system studied is a 2D sheet of nonlocal electron magnetoplasma embedded in a semi-infinite semiconductor medium with optical phonons. We examine the longitudinal collective mode spectrum as a function of distance z_0 of the 2D sheet from the bounding surface of the semiconductor. In particular, the 2D magnetoplasma/Bernstein modes couple preferentially to the bulk LO-phonon deep in the medium ($z_0 \rightarrow \infty$), whereas in the vicinity of the surface ($z_0 \rightarrow 0$) they couple preferentially to the surface phonon. This study is carried out by explicitly inverting the spatially inhomogeneous dielectric function of the combined system of a planar quantum-well plasma and a semi-infinite semiconductor in a position representation. The resulting closed-form inverse dielectric function $K(z_1, z_2)$ yields the oscillator strengths of the various modes as its position-dependent residues at the frequency poles defining the modes. [S0163-1829(99)10703-3]

I. INTRODUCTION: INVERSE DIELECTRIC FUNCTION

Advances in the fabrication of semiconductor nanostructures have focused considerable attention on collective modes in confined geometries, and much theoretical and experimental work has ensued. While many confined collective modes have already been studied, there are, in fact, yet more to be examined, particularly in the arena of confined collective modes in mutual interaction with one another. In this paper, we will investigate the interaction of two-dimensional (2D) Bernstein modes and the principal 2D magnetoplasmon with surface optical phonons as well as with bulk optical

phonons. Interest in this problem has been spurred by recent experimental observations,¹ and the need to explore the limits of validity of earlier theoretical work² which omitted treatment of the surface phonons. The system under consideration is depicted in Fig. 1, with a 2D sheet of magnetoplasma embedded in a semi-infinite host medium bearing optical phonons, the 2D sheet being parallel to and at a distance z_0 from the bounding surface of the host material. The magnetic field is perpendicular to both the interface and the plane of the 2D plasma sheet. The inverse dielectric function for this geometrical arrangement was derived recently,³ and it may be written in the form

$$K(z_1, z_2) = \frac{1}{\eta_+(z_1)} \left\{ \delta(z_1 - z_2) - \delta(z_2) \Gamma \eta_-(z_1) e^{-k|z_1|} - \frac{4\pi\alpha_0^{2D}(\vec{k}, \omega)}{\epsilon\Delta} [\delta(z_2 - z_0) - \delta(z_2) \Gamma e^{-kz_0}] \times [e^{-k|z_1 - z_0|} - \Gamma \eta_-(z_1) e^{-k|z_1|} e^{-kz_0}] \right\}, \quad (1.1)$$

where $K(z_1, z_2)$ is the Fourier transform of the inverse dielectric function $K(z_1, z_2, \vec{r}_1 - \vec{r}_2, t_1 - t_2)$ in the lateral plane $\vec{r}_1 - \vec{r}_2 \rightarrow \vec{k}$ and in time $t_1 - t_2 \rightarrow \omega$ with the appearance of both \vec{k} and ω suppressed. In Eq. (1.1), $\theta(z)$ is the Heaviside unit step function, and

$$\epsilon\Delta = \epsilon + 4\pi\alpha_0^{2D}(1 - \Gamma e^{-2kz_0}), \quad (1.2)$$

$$\eta_+(z) = \epsilon\theta(z) + \epsilon'\theta(-z), \quad (1.3)$$

$$\eta_-(z) = \theta(z) - \theta(-z), \quad (1.4)$$

and the dynamic host medium dielectric function incorporating optical phonons is

$$\epsilon \equiv \epsilon(\omega) = \epsilon_\infty \frac{\omega^2 - \omega_L^2}{\omega^2 - \omega_T^2}. \quad (1.5)$$

Here, ω_T and ω_L are the transverse- and longitudinal-optical-phonon frequencies, and ϵ_∞ is the high-frequency dielectric

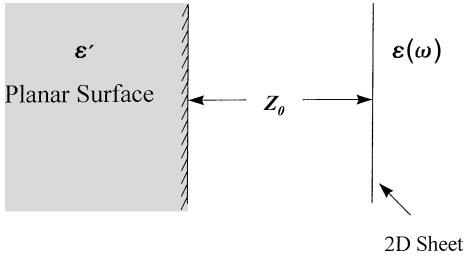


FIG. 1. Schematic of the 2D sheet at a distance z_0 from the interface at $z=0$ of a semi-infinite medium.

constant, while the adjoining medium dielectric constant is ϵ' . Furthermore, the image strength factor associated with the interface is

$$\Gamma \equiv \Gamma(\omega) = \frac{\epsilon' - \epsilon(\omega)}{\epsilon' + \epsilon(\omega)}. \quad (1.6)$$

Equation (1.1) represents a generalization of the results of Ref. 3 in several respects: (a) The in-plane polarizability $4\pi\alpha_0^{2D} = 4\pi\alpha_0^{2D}(\vec{k}, \omega)$ now includes nonlocal, as well as local, 2D structure and magnetic-field dependences, and (b) the adjoining medium dielectric constant is ϵ' (arbitrary) and is not restricted to the vacuum value unity. Moreover, (c) ϵ is still local and is taken to describe optical phonons of the bulk medium, as given by Eq. (1.5), instead of a plasma background of the host medium.

II. DISPERSION RELATION FOR COUPLED 2D MAGNETOPLASMONS AND SURFACE/BULK OPTICAL PHONONS

The longitudinal collective mode dispersion relation which emerges from Eq. (1.1) is given by

$$\omega_{\pm}^2 = \frac{1}{2} \left(\omega_L^2 + \omega_c^2 + \frac{\omega_{2D}^2}{\epsilon_{\infty}} \right) \pm \frac{1}{2} \sqrt{\left(\omega_L^2 + \omega_c^2 + \frac{\omega_{2D}^2}{\epsilon_{\infty}} \right)^2 - 4 \left(\omega_L^2 \omega_c^2 + \frac{\omega_{2D}^2 \omega_T^2}{\epsilon_{\infty}} \right)}. \quad (2.5)$$

Furthermore, we note that, deep in the medium, Eqs. (2.1) and (2.2) are also satisfied by $\epsilon' + \epsilon(\omega) = 0$, representing a surface phonon, $\omega_s^2 = [\epsilon' \omega_T^2 + \epsilon_{\infty} \omega_L^2] / [\epsilon' + \epsilon_{\infty}]$, completely decoupled from the modes of the distant 2D sheet.

2. 2D electron sheet near interface

Here $z_0 \rightarrow 0$ ($kz_0 \ll 1$): In this case the dispersion relation (2.2) takes the form

$$\epsilon \left(\frac{\epsilon' + \epsilon}{2} + 4\pi\alpha_0^{2D} \right) = 0. \quad (2.6)$$

The local mode arising from $\epsilon = 0$ is just the uncoupled bulk phonon, $\omega^2 = \omega_L^2$. It is clear from the vanishing of the second factor of Eq. (2.6) that the 2D magnetoplasmon preferentially couples to the surface phonon at $z_0 = 0$, through the quadratic dispersion relation

$$\frac{\epsilon' + \epsilon}{2} + 4\pi\alpha_0^{2D} = 0, \quad (2.7)$$

which yields the interacting local modes as

$$\omega_{\pm}^2 = \frac{1}{2} \left(\omega_s^2 + \omega_c^2 + \frac{\omega_{2D}^2}{\langle \epsilon \rangle} \right) \pm \frac{1}{2} \sqrt{\left(\omega_s^2 + \omega_c^2 + \frac{\omega_{2D}^2}{\langle \epsilon \rangle} \right)^2 - 4 \left(\omega_L^2 \omega_s^2 + \frac{\omega_{2D}^2 \omega_T^2}{\langle \epsilon \rangle} \right)}, \quad (2.8)$$

$$\epsilon \Delta \equiv \epsilon(\omega) + 4\pi\alpha_0^{2D}(1 - \Gamma e^{-2kz_0}) = 0, \quad (2.1)$$

which can alternatively be written as

$$\frac{\epsilon' + \epsilon(\omega)}{\epsilon' - \epsilon(\omega)} = \frac{4\pi\alpha_0^{2D} e^{-2kz_0}}{\epsilon(\omega) + 4\pi\alpha_0^{2D}}. \quad (2.2)$$

Two geometric limits which are of special interest will be discussed in detail in the following subsections, namely, when the 2D sheet is deep in the medium, $kz_0 \rightarrow \infty$, and when it is close to the interface, $kz_0 \rightarrow 0$.

A. Local spectrum

1. 2D electron sheet deep in the medium

Here $z_0 \rightarrow \infty$ ($kz_0 \gg 1$): In this case the dispersion relation (2.1) yields

$$\epsilon(\omega) + 4\pi\alpha_0^{2D} = \epsilon_{\infty} \frac{\omega^2 - \omega_L^2}{\omega^2 - \omega_T^2} + 4\pi\alpha_0^{2D} = 0, \quad (2.3)$$

which is independent of the bounding surface due to the large separation of the 2D sheet from the interface. In the local limit,^{4,5} $4\pi\alpha_0^{2D} = -\omega_{2D}^2 / [\omega^2 - \omega_c^2]$ (here $\omega_{2D}^2 = 2\pi n_{2D} e^2 k / m$, n_{2D} is the 2D density, and ω_c is the cyclotron frequency), this dispersion relation couples the 2D principal longitudinal magnetoplasmon ($\omega^2 \rightarrow \omega_c^2 + \omega_{2D}^2 / \epsilon_{\infty}$) with the bulk phonon ($\omega^2 = \omega_L^2$) through the quadratic relation

$$\epsilon_{\infty} \frac{\omega^2 - \omega_L^2}{\omega^2 - \omega_T^2} - \frac{\omega_{2D}^2}{\omega^2 - \omega_c^2} = 0, \quad (2.4)$$

which yields the interacting local modes ω_{\pm} as

where the constant $\langle \varepsilon \rangle$, defined as the average $\langle \varepsilon \rangle = (\varepsilon_\infty + \varepsilon')/2$, is effective in screening the 2D plasmon at the interface (whereas this screening role is played by ε_∞ deep in the medium).

B. Nonlocal spectrum

Admitting nonlocality to consideration introduces 2D Bernstein mode phenomenology into the dispersion relation [Eq. (2.2)] due to the occurrence of frequency poles of the 2D polarizability at multiples of the cyclotron frequency,^{5,6}

$$4\pi\alpha_0^{2D} = -\frac{4e^2m\omega_c}{k} \sum_{n=1}^{\infty} \frac{n\omega_c Z^{(n)}}{\omega^2 - [n\omega_c]^2}, \quad (2.9)$$

where $Z^{(n)}$ is given in Refs. 5 and 6 for all statistical regimes and magnetic-field strengths. In the illustrative calculations of the accompanying figures, we consider a nondegenerate 2D Landau-quantized plasma, for which ($\beta = 1/kT$ and $\Lambda^2 = \hbar k^2/2m\omega_c$)

$$Z^{(n)} = \frac{2\pi n_{2d}}{m\hbar\omega_c} \sinh\left(\frac{n\hbar\omega_c\beta}{2}\right) \times \exp\left[-\Lambda^2 \coth\left(\frac{\hbar\omega_c\beta}{2}\right)\right] I_n\left(\frac{\Lambda^2}{\sinh\hbar\omega_c\beta/2}\right). \quad (2.10)$$

For our purposes, it suffices to consider just one Bernstein mode in the vicinity of the frequency pole of the 2D polarizability at $2\omega_c$, in addition to the principal 2D magnetoplasmon, so we retain only the $n=1$ and 2 terms of the sum in Eq. (2.9), which is a good approximation for low wave number, $\Lambda^2 < \sinh(\hbar\omega_c\beta/2)$,

$$4\pi\alpha_0^{2D} \approx -\frac{\omega_{2D}^2}{\omega^2 - \omega_c^2} - \frac{\Omega_k^2}{\omega^2 - (2\omega_c)^2}, \quad (2.11)$$

where^{5,6} $\Omega_k^2 \equiv 2\pi e^2 \sigma_{2D} k^3 / m^2 \omega_c^2$ and $\sigma_{2D} = (\hbar\omega_c n_{2D}/2) \coth(\hbar\omega_c\beta/2)$.

1. $z_0 \rightarrow \infty$

It follows that for the 2D electron sheet deep in the medium Eq. (2.4) is supplanted by

$$\frac{\omega^2 - \omega_L^2}{\omega^2 - \omega_T^2} - \frac{\omega_{2D}^2/\varepsilon_\infty}{\omega^2 - \omega_c^2} - \frac{\Omega_k^2/\varepsilon_\infty}{\omega^2 - (2\omega_c)^2} = 0. \quad (2.12)$$

This dispersion relation, which is cubic in ω^2 , can be solved exactly analytically, but it is cumbersome, and we therefore provide approximate solutions which correspond to the coupled modes ω_\pm [Eq. (2.5)] of the 2D principal-longitudinal-magnetoplasmon/bulk-phonon type in weak interaction with the Bernstein mode $n=2$. The mutual shifting of these modes due to this weak interaction is readily determined by rewriting Eq. (2.12) in the form

$$(\omega^2 - \omega_+^2)(\omega^2 - \omega_-^2) = \frac{(\Omega_k^2/\varepsilon_\infty)(\omega^2 - \omega_T^2)(\omega^2 - \omega_c^2)}{\omega^2 - (2\omega_c)^2}, \quad (2.13)$$

from which we have the weakly coupled modes $\tilde{\omega}_\pm$ deep in the medium as (approximately)

$$\tilde{\omega}_\pm^2 \approx \omega_\pm^2 + \frac{(\Omega_k^2/\varepsilon_\infty)(\omega_\pm^2 - \omega_T^2)(\omega_\pm^2 - \omega_c^2)}{(\omega_\pm^2 - \omega_\mp^2)[\omega_\pm^2 - (2\omega_c)^2]}, \quad (2.14)$$

and within this framework the $n=2$ Bernstein mode $\tilde{\omega}_{n=2}$ is given by

$$\tilde{\omega}_{n=2}^2 \approx (2\omega_c)^2 + \frac{(\Omega_k^2/\varepsilon_\infty)[(2\omega_c)^2 - \omega_T^2](3\omega_c^2)}{[(2\omega_c)^2 - \omega_+^2][(2\omega_c)^2 - \omega_-^2]}. \quad (2.15)$$

Again, there is another mode deep in the medium, namely, the decoupled surface phonon at ω_s , as discussed after Eq. (2.5), for a total of four modes. These approximations, which apply for $z_0 \rightarrow \infty$, are not valid when the $n=2$ Bernstein mode is in a parameter range of strong interaction with ω_+ or ω_- .

2. $z_0 \rightarrow 0$

In the case when the 2D electron sheet is near the interface, the dispersion relation [Eq. (2.7)] for the coupled modes ω_\pm [Eq. (2.8)] is supplanted by

$$(\omega^2 - \omega_+^2)(\omega^2 - \omega_-^2) = \frac{2\Omega_k^2 \omega^2 (\omega^2 - \omega_T^2)}{(\varepsilon' + \varepsilon_\infty)[\omega^2 - (2\omega_c)^2]}. \quad (2.16)$$

In the parameter ranges of weak interaction between the $n=2$ Bernstein mode and ω_\pm , we have approximate solutions $\tilde{\omega}_\pm$ for $z_0 \rightarrow 0$ as

$$\tilde{\omega}_\pm^2 = \omega_\pm^2 + \frac{2\Omega_k^2}{\varepsilon' + \varepsilon_\infty} \frac{\omega_\pm^2 (\omega_\pm^2 - \omega_T^2)}{[\omega_\pm^2 - (2\omega_c)^2](\omega_\pm^2 - \omega_\mp^2)}, \quad (2.17)$$

and the $n=2$ Bernstein mode $\tilde{\omega}_{n=2}$ is approximately

$$\tilde{\omega}_{n=2}^2 = (2\omega_c)^2 + \frac{2\Omega_k^2}{\varepsilon' + \varepsilon_\infty} \frac{4\omega_c^2 [(2\omega_c)^2 - \omega_T^2]}{[(2\omega_c)^2 - \omega_+^2][(2\omega_c)^2 - \omega_-^2]}. \quad (2.18)$$

The fourth mode at $z_0 \rightarrow 0$ is the decoupled bulk phonon at ω_L , as discussed after Eq. (2.6). Again, these results for $z_0 \rightarrow 0$ are not valid for parameter ranges when the $n=2$ Bernstein mode is in strong interaction with ω_+ or ω_- .

III. EXCITATION AMPLITUDES: OSCILLATOR STRENGTHS

It is also important to provide information about the excitation amplitudes of the coupled modes we have examined. These excitation amplitudes, or oscillator strengths, are given by the residues of $K(z_1, z_2)$ at the frequency pole positions of the collective modes of the coupled system, and we determine them using Eqs. (1.1), (1.2), etc., for the case when the 2D Bernstein mode $\tilde{\omega}_{n=2}$ is weakly coupled to $\tilde{\omega}_\pm$ as follows (below, *Res* denotes residue).

(1) When the 2D sheet is deep in the medium, $z_0 \rightarrow \infty$, we have

$$Res K(z_1, z_2)_{\omega \rightarrow \tilde{\omega}_{\pm}} = \frac{(\tilde{\omega}_{\pm}^2 - \omega_T^2)(\tilde{\omega}_{\pm}^2 - \omega_c^2)[\tilde{\omega}_{\pm}^2 - (2\omega_c)^2]}{\eta_+(z_1)\varepsilon_{\infty}(2\tilde{\omega}_{\pm})(\tilde{\omega}_{\pm}^2 - \tilde{\omega}_{\mp}^2)(\tilde{\omega}_{\pm}^2 - \tilde{\omega}_{n=2}^2)} \left(\frac{\omega_{2D}^2}{\tilde{\omega}_{\pm}^2 - \omega_c^2} + \frac{\Omega_k^2}{\tilde{\omega}_{\pm}^2 - (2\omega_c)^2} \right) \delta(z_2 - z_0) e^{-k|z_1 - z_0|} \quad (3.1)$$

and

$$Res K(z_1, z_2)_{\omega \rightarrow \tilde{\omega}_{n=2}} = \frac{(\tilde{\omega}_{n=2}^2 - \omega_T^2)(\tilde{\omega}_{n=2}^2 - \omega_c^2)[\tilde{\omega}_{n=2}^2 - (2\omega_c)^2]}{\eta_+(z_1)\varepsilon_{\infty}(\tilde{\omega}_{n=2}^2 - \tilde{\omega}_{+}^2)(\tilde{\omega}_{n=2}^2 - \tilde{\omega}_{-}^2)(2\tilde{\omega}_{n=2})} \left(\frac{\omega_{2D}^2}{\tilde{\omega}_{n=2}^2 - \omega_c^2} + \frac{\Omega_k^2}{\tilde{\omega}_{n=2}^2 - (2\omega_c)^2} \right) \delta(z_2 - z_0) e^{-k|z_1 - z_0|}, \quad (3.2)$$

where $\tilde{\omega}_{\pm}, \tilde{\omega}_{n=2}$ are given by Eqs. (2.14) and (2.15), respectively.

(2) When the 2D sheet is near the interface, $z_0 \rightarrow 0$, we have

$$Res K(z_1, z_2)_{\omega \rightarrow \tilde{\omega}_{\pm}} = -\frac{4\pi\alpha_0^{2D}}{\eta_+(z_1)} [\delta(z_2 - z_0) - \delta(z_2)\Gamma(\tilde{\omega}_{\pm})][1 - \Gamma(\tilde{\omega}_{\pm})\eta_-(z_1)] e^{-k|z_1|} \\ \times \left(\frac{[\varepsilon' + \varepsilon(\tilde{\omega}_{\pm})](\tilde{\omega}_{\pm}^2 - \omega_T^2)(\tilde{\omega}_{\pm}^2 - \omega_c^2)[\tilde{\omega}_{\pm}^2 - (2\omega_c)^2]}{(\varepsilon' + \varepsilon_{\infty})\varepsilon(\omega_{\pm})(\tilde{\omega}_{\pm}^2 - \tilde{\omega}_{\mp}^2)(2\tilde{\omega}_{\pm})(\tilde{\omega}_{\pm}^2 - \tilde{\omega}_{n=2}^2)} \right) \quad (3.3)$$

and

$$Res K(z_1, z_2)_{\omega \rightarrow \tilde{\omega}_{n=2}} = -\frac{4\pi\alpha_0^{2D}}{\eta_+(z_1)} [\delta(z_2 - z_0) - \delta(z_2)\Gamma(\tilde{\omega}_{n=2})][1 - \Gamma(\tilde{\omega}_{n=2})\eta_-(z_1)] e^{-k|z_1|} \\ \times \left(\frac{[\varepsilon' + \varepsilon(\tilde{\omega}_{n=2})](\tilde{\omega}_{n=2}^2 - \omega_T^2)(\tilde{\omega}_{n=2}^2 - \omega_c^2)[\tilde{\omega}_{n=2}^2 - (2\omega_c)^2]}{(\varepsilon' + \varepsilon_{\infty})\varepsilon(\omega_{n=2})(\tilde{\omega}_{n=2}^2 - \tilde{\omega}_{+}^2)(\tilde{\omega}_{n=2}^2 - \tilde{\omega}_{-}^2)(2\tilde{\omega}_{n=2})} \right), \quad (3.4)$$

where $\tilde{\omega}_{\pm}, \tilde{\omega}_{n=2}$ are given in this case by Eqs. (2.17) and (2.18), respectively, in the parameter ranges of weak interaction of the modes.

In Eqs. (3.1)–(3.4), we have focused on the residues of the collective modes which involve coupling of the 2D principal magnetoplasmon and phonon modes with the Bernstein mode $n=2$. Terms involving $\delta(z_2)$ reflect the fact that the surface modes can only be excited by an impressed field impinging directly on the interface, (in the local limit considered for the host medium) and terms involving $\delta(z_2 - z_0)$ require impressed fields to impinge directly on the 2D electron sheet to excite 2D magnetoplasmons. The factors $e^{-k|z_1 - z_0|}$ and $e^{-k|z_1|}$ describe the effective electrostatic potential at z_1 in accordance with the Poisson equation.

IV. CONCLUSIONS: z_0 -GEOMETRY DEPENDENCE OF THE COMBINED INTERACTING MODE SPECTRUM

The results above indicate that the 2D magnetoplasma mode and $n=2$ Bernstein mode couple preferentially to the bulk phonon ω_L when the 2D plasma sheet is deep in the medium ($kz_0 \gg 1$), but when it is near the bounding surface ($kz_0 \ll 1$) the 2D electron magnetoplasma oscillations couple preferentially to the surface phonon ω_s . To gain an appreciation of how the longitudinal coupled modes hybridize and behave over the entire z_0 range, and to examine parameter regimes in which the $n=2$ Bernstein mode interacts strongly with ω_+ or ω_- , we analyze the z_0 -dependent longitudinal dispersion relation of Eq. (2.2) numerically. Generally speaking, such regimes of strong interaction of the Bernstein

mode occur when Ω_k is comparable to the other characteristic frequencies of the system, such as ω_{2D} and ω_L , and/or there is a ‘‘crossover’’ of $2\omega_c$ with the other characteristic frequencies (which would occur in the absence of such interactions).

The dispersion relation for arbitrary z_0 given by Eqs. (2.1) or (2.2), taken jointly with Eq. (2.11) for the nonlocal Landau-quantized 2D polarizability at low wave number, is quartic in ω^2 . This yields four nonlocal collective modes shown in Figs. 2 and 3. In Fig. 2, we chose $z_0 = 20 \text{ \AA}$ and $B = 12 \text{ T}$ for a GaAs-based quantum well, exhibiting the dispersion of the four mode frequencies ω/ω_L as a function of wave number $k/\sqrt{2\pi n_{2D}}$ for a nondegenerate 2D Landau-quantized plasma of density $n_{2D} = 10^{12}/\text{cm}^2$. It is clear that there is considerable interaction among the nonlocal ω_+ , ω_- , and $n=2$ Bernstein modes, with mutual repulsion of the modes in their wave-number variation. The fourth ‘‘phonon’’ mode (almost independent of wave number) is limited to the decoupled surface phonon ω_s as z_0 becomes large. In Fig. 3, the four mode frequencies ω/ω_L are plotted as functions of z_0 (\AA) for $k/\sqrt{2\pi n_{2D}} = 0.2$ and $B = 12 \text{ T}$. In these calculations, we took the Al composition as $x_c = 0.3$, and used⁷ $\varepsilon' = 13.18 - 3.12x_c$, $\varepsilon_{\infty} = 10.89 - 2.73x_c$, and the electron effective mass $m/m_0 = 0.0665(1 - x_c) + 0.15x_c$, $\omega_L = (36.25 - 6.55x_c + 1.79x_c^2) \text{ meV}$, and $\omega_T = (33.29 - 0.64x_c - 1.16x_c^2) \text{ meV}$. Again, we have the nonlocal ω_+ and ω_- modes, with the ω_+ mode having a greater variation with z_0 than does the ω_- mode. The $n=2$ Bernstein mode is seen to be almost independent of z_0 , and the fourth ‘‘phonon’’ mode limits to the decoupled bulk-phonon frequency ω_L as $z_0 \rightarrow 0$, while approaching the decoupled

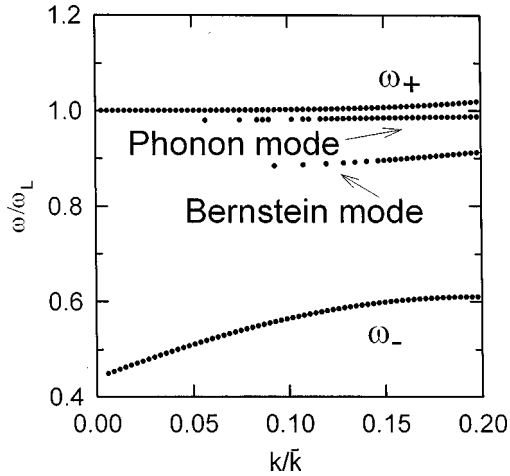


FIG. 2. Plot of the eigenmode frequencies, in units of the longitudinal bulk-phonon frequency ω_L , as functions of k/\bar{k} where $\bar{k} = (2\pi n_{2D})^{1/2}$, for $z_0 = 20 \text{ \AA}$ and $B = 12 \text{ T}$. The GaAs parameters used in the calculation are given in the text, as is ϵ' for the adjacent medium.

surface-phonon frequency ω_s as $z_0 \rightarrow \infty$. Since $\omega_s^2 = (\epsilon' \omega_T^2 + \epsilon_\infty \omega_L^2) / (\epsilon' + \epsilon_\infty)$ differs only slightly from ω_L^2 for GaAs/ $\text{Al}_x\text{Ga}_{1-x}\text{As}$, this ‘‘phonon’’ mode is almost flat, varying by about 20% as z_0 ranges over 100 \AA . Correspondingly, the coupling of the Bernstein mode to the surface phonon is hard to distinguish from its coupling to the bulk phonon in the case of GaAs/ $\text{Al}_x\text{Ga}_{1-x}\text{As}$.

To explore the lack of variation of the Bernstein mode as a function of z_0 , we have considered changing the adjacent medium so that ϵ' differs greatly from ϵ , choosing an ideal metal $\epsilon' \rightarrow -\infty$. In this case our analysis of Eq. (2.1) yields three eigenmodes, which are plotted as functions of $k/\sqrt{2\pi n_{2D}}$ in Fig. 4 for fixed $z_0 = 20 \text{ \AA}$ and $B = 12 \text{ T}$. The plot of the three modes as functions of z_0 in Fig. 5 for fixed $k/\sqrt{2\pi n_{2D}} = 0.2$ shows an increased variation of ω_- with z_0 , and somewhat less variation of ω_+ . (The parameters used in the numerical calculations for Figs. 4 and 5 are the same as

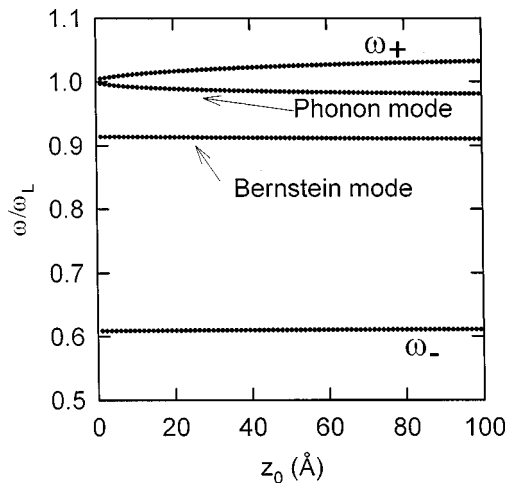


FIG. 3. Plot of the eigenmode frequencies, in units of the longitudinal bulk-phonon frequency ω_L , as functions of the distance z_0 of the 2D sheet from the interface at $z=0$ for $k/\bar{k} = 0.2$ and $B = 12 \text{ T}$. All other parameters are the same as in Fig. 2.

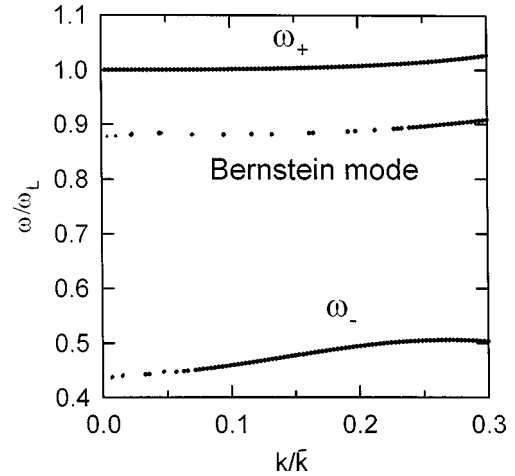


FIG. 4. Same as in Fig. 2, except that $\epsilon' = -\infty$.

those used for Figs. 2 and 3, except that $\epsilon' \rightarrow -\infty$.) The Bernstein mode of Fig. 5 shows greater variation with z_0 in this case than was seen above. It is of particular interest to note that the ‘‘phonon’’ mode, which varied from ω_L to ω_s above, is now absent. As indicated above, in the present case of an adjacent ideal metal,

$$\frac{1}{\Gamma} = \frac{\epsilon' + \epsilon(\omega)}{\epsilon' - \epsilon(\omega)} \rightarrow 1, \quad (4.1)$$

the dispersion relation of Eqs. (2.1) and (2.2) is cubic, not quartic, in ω^2 , having only the three roots shown in Figs. 4 and 5. Physically, the impossibility of a fourth mode is underscored by Eq. (4.1), which clearly rules out the existence of a surface mode corresponding to $\epsilon' + \epsilon(\omega) \rightarrow 0$.

In summary, the geometry dependence of the coupled collective mode spectrum arising from 2D magnetoplasmon/Bernstein modes in interaction with surface and bulk phonons has been examined here. We have also shown that the coupled modes are accompanied by a position-geometry dependence of their relative excitation amplitudes (oscillator strengths), as described in Sec. III above. These explicit and detailed results show that the 2D magnetoplasma/Bernstein modes couple preferentially to the bulk LO phonon when

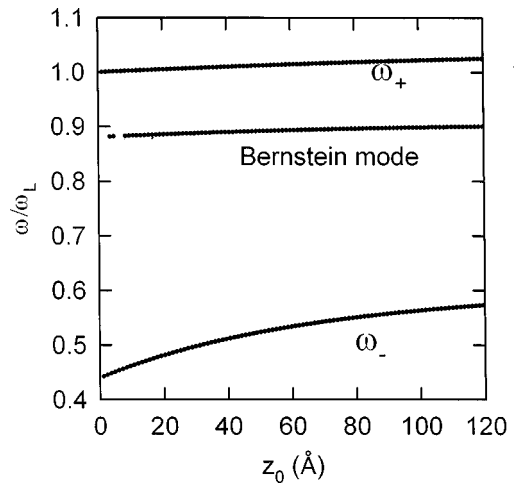


FIG. 5. Same as in Fig. 3 except that $\epsilon' = -\infty$.

$z_0 \rightarrow \infty$, deep in the medium, whereas, in the vicinity of the interface, $z_0 \rightarrow 0$, they couple preferentially to the surface phonon. One may expect a greater variation of the $n=2$ Bernstein mode as a function of z_0 for materials of relatively low mass, which puts $2\omega_c$ directly in the region of interac-

tion with ω_{\pm} , and which also have a larger difference between ω_T and ω_L than that of GaAs/Al_xGa_{1-x}As (so that the surface phonon differs more substantially from the bulk phonon in its coupling with the Bernstein mode). One such possible material choice is a HgTe-based quantum well.

*Also at The Graduate School and University Center of the City University of New York, 33 West 42nd Street, New York, NY 10036.

¹D. E. Bangert, R. J. Stuart, H. P. Hughes, D. A. Richter, and J. E. F. Frost, *Semicond. Sci. Technol.* **11**, 352 (1996).

²V. L. Gurevich and K. E. Shtengl, *J. Phys.: Condens. Matter* **2**, 6323 (1990).

³N. J. M. Horing, T. Jena, H. L. Cui, and J. D. Mancini, *Phys.*

Rev. B **54**, 2785 (1996).

⁴N. J. M. Horing and M. Yildiz, *Phys. Lett.* **44A**, 386 (1973).

⁵N. J. M. Horing, M. Orman, and M. Yildiz, *Phys. Lett.* **48A**, 7 (1974).

⁶N. J. M. Horing, M. Orman, E. Kamen, and M. L. Glasser, *Phys. Lett.* **85A**, 378 (1981).

⁷S. Adachi, *J. Appl. Phys.* **58**, R1 (1985).